Geophysical Prospecting **39**, 803–826, 1991

ASPECTS OF CHARGE ACCUMULATION IN d.c. RESISTIVITY EXPERIMENTS[1]

YAOGUO LI and DOUGLAS W. OLDENBURG[2]

ABSTRACT

LI, Y. and OLDENBURG, D.W. 1991. Aspects of charge accumulation in d.c. resistivity experiments. *Geophysical Prospecting* **39**, 803–826.

When an electric current is introduced to the earth, it sets up a distribution of charges both on and beneath the earth's surface. These charges give rise to the anomalous potential measured in the d.c. resistivity experiment. We investigate different aspects of charge accumulation and its fundamental role in d.c. experiments. The basic equations and boundary conditions for the d.c. problem are first presented with emphasis on the terms involving accumulated charges which occur wherever there is a non-zero component of electric field parallel to the gradient of conductivity. In the case of a polarizable medium, the polarization charges are also present due to the applied electric field, yet they do not change the final field distribution. We investigate the precise role of the permittivity of the medium. The charge buildup alters the electric fields and causes the refraction of current lines; this results in the well-known phenomenon of current channelling. We demonstrate this by using charge density to derive the refraction formula at a boundary. An integral equation for charge density is presented for whole-space models where the upper half-space is treated as an inhomogeneity with zero conductivity. The integral equation provides a tool with which the charge accumulation can be examined quantitatively and employed in the practical forward modelling. With the aid of this equation, we investigate the effect of accumulated charges on the earth's surface and show the equivalence between the half-space and whole-space formulations of the problem. Two analytic examples are presented to illustrate the charge accumulation and its role in the d.c. problem. We investigate the relationship between the solution for the potential via the image method and via the charge density. We show that the essence of the image method solution to the potential problem is to derive a set of fictitious sources which produce the same potential as does the true charge distribution. It follows that the image method is viable only when the conductivity structure is such that the effect of the accumulated charge can be represented by a set of point images. As numerical examples, we evaluate quantitatively the charge density on the earth's surface that arises because of topography and the charge density on a buried conductive prism. By these means, we demonstrate the use of the boundary element technique and charge density in d.c. forward modelling problems.

[1] Received October 1989, last material received February 1991.

[2] Department of Geophysics and Astronomy, University of British Columbia, 129-2219 Main Mall, Vancouver, B.C., Canada V6T 1W5.

INTRODUCTION

In d.c. resistivity experiments, all information about the underground geo-electrical structure is contained in observed potential differences measured at the earth's surface or at depth. The measured potential arises from two sources: (1) the potential due to a current source embedded in a half-space of conductivity equal to that of the region immediately surrounding the current electrode; and (2) the potential that arises from volumetric and surface charge distributions which are set up in the medium. The existence and distribution of these charges in the earth and on the earth's surface are fundamental to d.c. potential signals and it follows that a thorough understanding of charge accumulation should provide enhanced insight into the forward modelling of d.c. potentials and in formulating new approaches to the inversion of d.c. data.

The concept and importance of charge accumulation in d.c. conduction problems are certainly not new and the physical principles, associated mathematics and numerical results have been detailed in many papers. Alpin (1947) was perhaps the first to point out that the source of potential in d.c. experiments is accumulated charge. His seminal paper presents the physical interpretation and basic mathematical description of the electric field in a conductive medium using charge accumulation and it also presents an integral equation for the surface charge density. Alfano (1959, 1960, 1961) provides a comprehensive treatment of modelling and interpreting d.c. resistivity data using charge accumulation. His presentation gives a basic understanding of the field behaviour that arises in the presence of conductivity discontinuities in an orthogonally gridded 3D environment. Basic physical equations relating to the accumulation of electric charge in a conductive medium and evaluation of electric potentials from boundary charges are lucidly developed in the excellent work of Kaufman and Keller (1985, pp. 11–44). Kaufman (1985) presents a tutorial dissertation regarding the role of charge buildup in time-varying problems which contains insight and physical understanding about the d.c. limit that we are interested in here. The use of charge density in correcting for the effects of topographic distortion is examined by Oppliger (1984). Jiracek (Lecture at 9th workshop on EM induction, Sochi, 1988) investigates the distortion of EM measurements due to the charge accumulation resulting from topography and near-surface variation. Finally, integral equations for the d.c. problem have been derived and used in forward modelling by numerous authors (e.g. Dieter, Paterson and Grant 1969; Snyder 1976; Okabe 1984). Integral equation forward modelling approaches have their computation divided into two parts. The first computes the charge density on boundaries of blocks across which there is a conductivity contrast, and the second uses Coulomb's law to compute the potential at the observer site that arises from this charge. This division tends to emphasize the importance and the physical role of charge accumulation.

Despite the existence of the above works (and numerous others not mentioned which treat various aspects of charge density in d.c. resistivity problems) we have not found a reference in which all the aspects of charge density in which we were interested were outlined. As such, we felt that there is a need for a paper which is devoted explicitly to aspects and ramifications of charge density buildup in d.c.

problems. We concede that much of the mathematics and physical insight that is presented here can be found in the literature. Our goal, however, has been to assimilate some of this diverse information into a single document, enlarge it with our own insight, and present results in a uniform notation. It is our hope that this paper is a lucid and concise summary of many aspects of charge accumulation and that it will be of use to others who are involved with interpreting d.c. measurements.

We begin with the governing equations and boundary conditions for d.c. potentials in a conducting medium; particular emphasis is paid to terms which involve charge density. The application of an electric field to a polarizable medium produces a polarization charge. Although it is generally well known that this charge does not alter the observed potentials, the precise role of the polarization charge is sometimes not appreciated and hence it is a source of confusion. We treat this aspect explicitly. We next look at the relationship between refraction of currents at a boundary and the change in the electric field caused by the surface charges. This emphasizes the fundamental role played by charge accumulation in current channelling problems. An integral equation for charge density is developed and solved with the aid of the whole-space Green's function. This illustrates how boundary element forward modelling results can be obtained and also suggests how topographic problems can be handled. Analytic expressions for charge density resulting from a buried current source in a half-space, and in a layer over a half-space, are derived using the integral equations. Since the image method is often used to solve simple d.c. problems, we outline the method here and show how this mathematical derivation relates to the physical aspects of charge accumulation. This analysis is conveniently illustrated by considering the potential in a two-layered earth. Lastly, we present some numerical examples to quantify the charge density buildup on a simple 2D topography and on a 3D body buried in a half-space.

Basic Equations

In a d.c. resistivity experiment current is input to the ground and potential differences are measured away from the source. The electric potential at any point in the medium is dependent upon the distribution of the conductivity within the earth and that potential may be evaluated by using Maxwell's equations, conservation laws, constitutive relations and the boundary conditions. We outline the basic equations and boundary conditions required to understand and to solve the d.c. problem. Equations which involve charge density are emphasized. The reader is referred to Stratton (1941), Grant and West (1965), Jeans (1966), Keller and Frischknecht (1966), Telford *et al.* (1976), Kaufman and Keller (1985, ch. 2) and Ward and Hohmann (1988) for additional material.

For a steady-state problem, only two of Maxwell's equations are needed:

$$\nabla \times \mathbf{E} = \mathbf{0} \tag{1}$$

and

$$\nabla \cdot \mathbf{D} = \rho_f, \tag{2}$$

where $\mathbf{E}$ is the electric field, $\mathbf{D}$, the electric displacement and ρ_f, the volumetric free charge density.

The law of conservation of charge states that

$$\nabla \cdot \mathbf{j} = -\frac{\partial \rho_f}{\partial t}, \tag{3}$$

where $\mathbf{j}$ is the current density due to free charges. Throughout this paper we define a positive current to be related to the flow of positive charge carriers. In steady-state conditions $\nabla \cdot \mathbf{j} = 0$ is satisfied everywhere except at locations of sources or sinks of electric charges. If a current I is injected at a location $\mathbf{r}_s$,

$$\nabla \cdot \mathbf{j} = I\delta(\mathbf{r} - \mathbf{r}_s). \tag{4}$$

In addition to field equations we also require constitutive relations. For the purpose of this paper, we assume that the medium is linear and isotropic. Thus

$$\mathbf{D} = \varepsilon \mathbf{E} \tag{5}$$

and

$$\mathbf{j} = \sigma \mathbf{E}, \tag{6}$$

where σ is the electric conductivity and ε is the permittivity.

Finally, at an interface separating media of different conductivities, the tangential component of the electric field and the normal component of current density are continuous. Thus

$$E_{1t} = E_{2t} \tag{7}$$

and

$$j_{1n} = j_{2n}, \tag{8}$$

where subscripts 1 and 2 refer to the respective media and subscripts t and n refer to tangential and normal components. The unit normal vector $\hat{\mathbf{n}}$ is chosen to point outwards from medium 1 at the interface (Fig. 1). The normal components of $\mathbf{D}$ and $\mathbf{E}$ satisfy

$$D_{2n} - D_{1n} = \tau_f \tag{9}$$

and

$$E_{2n} - E_{1n} = \frac{\tau_t}{\varepsilon_0}, \tag{10}$$

where τ_f and τ_t are respectively the surface densities of free and total charge. Thus the normal components of $\mathbf{D}$ and $\mathbf{E}$ can be discontinuous if there is a surface charge distribution on the boundary. Using (1) and the vector identity $\nabla \times \nabla\phi = \mathbf{0}$, we can

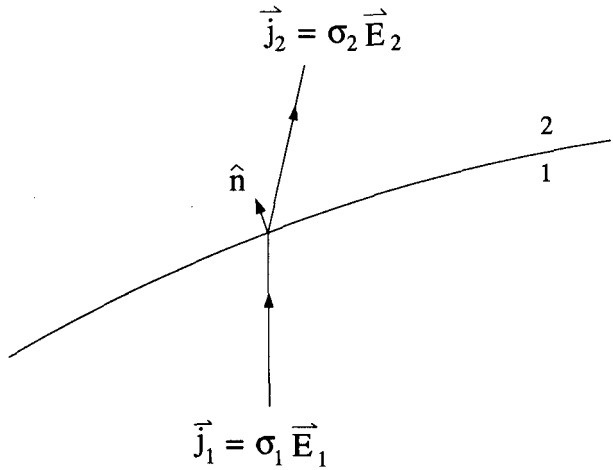

FIG. 1. Basic geometry for current flow at a boundary.

express the electric field as the gradient of a scalar potential ϕ,

$$\mathbf{E} = -\nabla\phi. \tag{11}$$

The electric field is bounded away from sources. Consequently, the potential is continuous and we have the boundary condition $\phi_1 = \phi_2$.

Any steady-state conduction problem can be solved using the above equations and boundary conditions. In the most general approach, substitution of (6) and (11) into (4) yields

$$\nabla \cdot (\sigma \nabla\phi) = -I\delta(\mathbf{r} - \mathbf{r}_s), \tag{12}$$

which can be expanded to produce

$$\nabla^2\phi = -\frac{\nabla\sigma \cdot \nabla\phi}{\sigma} - \frac{I}{\sigma}\delta(\mathbf{r} - \mathbf{r}_s). \tag{13}$$

We recognize (13) formally as Poisson's equation. The two terms on the right-hand side have units of ρ/ε_0 and therefore each can be thought of as charge density. For the purpose of calculating the potential, the term involving the source current can be replaced by an effective point charge of magnitude $Q = \varepsilon_0 I/\sigma_s$, where σ_s is the conductivity at the location of the current source. The first term on the right-hand side is of prime interest because it expresses the charge buildup that exists as a result of changes in the electrical conductivity structure. It is non-zero whenever there is a component of electric field parallel to the conductivity gradient. Under these conditions there will be a physical buildup of electric charge with volumetric density

$$\rho_t = \varepsilon_0 \frac{\nabla\sigma \cdot \nabla\phi}{\sigma}. \tag{14}$$

In the limit, when the conductivity gradient approaches infinity, i.e. when the medium suffers a discontinuous change in conductivity, the volumetric charge density in (14) becomes a surface charge density confined to the boundary separating the two regions. It is this charge which creates a discontinuity in the normal components of **D** and **E** as in (9) and (10).

By combining (8) and (10) and using Ohm's law, the charge density can be written as

$$\frac{\tau_t}{\varepsilon_0} = \left(1 - \frac{\sigma_2}{\sigma_1}\right) E_{2n}. \tag{15}$$

Equations (14) and (15) show that the accumulated charge is negative when current flows from a resistive into a conductive region. Conversely, positive charge accumulates when a current flows from a conductive to a resistive region. This rule, delineating the signs of the accumulated charge, is very useful for predicting the general character of d.c. fields resulting from simple geological structures.

A question relevant to understanding the charge buildup is related to the importance of permittivity of the conductive medium. Equation (13) indicates that conductivity is the governing parameter for a stationary electric field and that permittivity does not play a part. Yet, application of an electric field to a polarizable material creates polarization charges which produce an electric potential. This apparent contradiction is sometimes a source of confusion. It is best illustrated by examining what is happening on the boundary between two media.

An electric field applied to a polarizable medium generates an electric polarization or dipole moment per unit volume. The polarization is proportional to the applied total electric field, and is given by

$$\mathbf{P} = \chi \varepsilon_0 \mathbf{E}, \tag{16}$$

where **P** is the polarization vector, and $\chi = (\varepsilon/\varepsilon_0) - 1$ is the electric susceptibility. At the boundary of the medium there will be an polarization charge $\tau_b = \mathbf{P} \cdot \hat{\mathbf{n}}$, where $\hat{\mathbf{n}}$ is the normal vector. The net polarization charge density at a boundary separating media with permittivities ε_1 and ε_2 is

$$\tau_b = -(P_{2n} - P_{1n}), \tag{17}$$

and the total charge is the sum of this polarization charge plus the free charge. Substituting (6) into (9), and (16) into (17) and summing yields

$$\begin{aligned} \tau_t &= \tau_f + \tau_b \\ &= \varepsilon_0 (E_{2n} - E_{1n}), \end{aligned}$$

which is precisely the same as (10). It is this total charge density on the boundary which is responsible for the continuity of the normal component of the current density and this charge is not affected by variations in permittivity. The permittivity however, does determine how much free charge has to be accumulated at the boundary so that boundary conditions are satisfied.

In general, when the physical properties are changing continuously, a volumetric charge density of

$$\frac{\rho_t}{\varepsilon_0} = -\frac{\nabla\sigma \cdot \mathbf{E}}{\sigma}$$

is set up. Again, this charge density is determined only by the conductivity, but if the medium is polarizable, then ρ_t can be explicitly formed as the sum of free and polarization charge densities. The expressions for these are

$$\rho_f = -\frac{\varepsilon}{\sigma}\nabla\sigma \cdot \mathbf{E} + \mathbf{E} \cdot \nabla\varepsilon \tag{18}$$

and

$$\rho_b = (\varepsilon - \varepsilon_0)\frac{\nabla\sigma \cdot \mathbf{E}}{\sigma} - \mathbf{E} \cdot \nabla\varepsilon. \tag{19}$$

The sum of ρ_f and ρ_b gives the total charge density which determines the final electric field.

To summarize, in a d.c. experiment, electric charges accumulate whenever there is a gradient of conductivity and a non-zero component of electric field parallel to it. The final electric field is produced by the primary source and by surface and volumetric charge distributions. When the medium is polarizable, both free and polarization charges contribute to the total accumulated charge. However, the total accumulated charge is controlled only by electrical conductivity; the polarization plays no part other than to supply a portion of the charges needed to satisfy the boundary conditions.

Current Flow in d.c. Resistivity Problems

We are focusing upon the accumulated electric charges in order to provide insight about the d.c. resistivity problem. However, a common description of d.c. fields uses the concept of current flow. The variations in conductivity structure alter the flow of electric charges and the final distribution of current is such that the energy loss due to ohmic dissipation is minimized. Physically, this results in current being channelled into the regions of high conductivity and deflected away from resistive regions. But knowledge of the current distribution, or even its direction, does not imply immediate knowledge about the potentials. In particular, current direction at any point is determined by the gradient of the potential. Current magnitude also requires specification of an electrical conductivity.

The relationship between current flow and charge accumulation is best illustrated by considering the refraction, or change in direction, of currents impinging upon a plane interface separating two media. This refraction is a direct effect of surface charges which accumulate on the interface. We quantify this here but the reader is also referred to Kaufman and Keller (1985). Consider, as in Fig. 2a, a point on the boundary and let $\mathbf{E}_b$ be the base electric field which is produced by all sources away from this point. Continuity of the normal component of the current

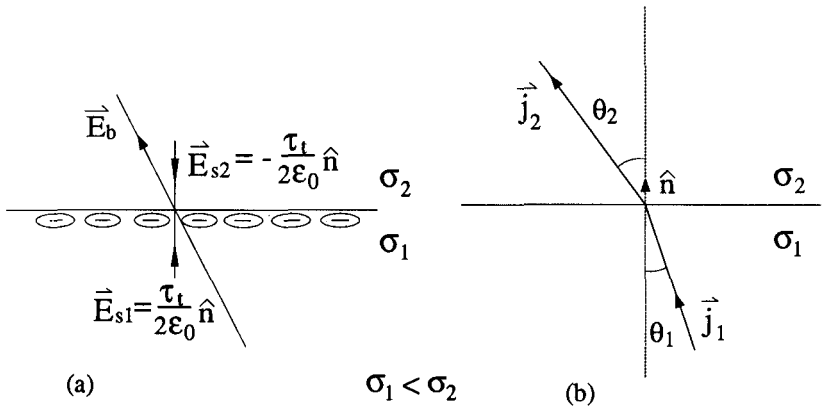

FIG. 2. (a) Electric charges accumulate on the boundary separating two conductive media and produce perturbation fields $\mathbf{E}_{s1}$ and $\mathbf{E}_{s2}$ normal to the boundary. These fields are added to the base field $\mathbf{E}_b$ to produce a total field whose direction changes at the boundary. The resultant current flow shown in (b) is equivalently refracted at the boundary.

density requires the existence of a charge density τ_t (given by (10)). This charge affects the normal components of the electric field at the immediate vicinity so that

$$E_{1n} = \mathbf{E}_b \cdot \hat{\mathbf{n}} - \frac{\tau_t}{2\varepsilon_0}$$

and (20)

$$E_{2n} = \mathbf{E}_b \cdot \hat{\mathbf{n}} + \frac{\tau_t}{2\varepsilon_0}.$$

An expression for the total accumulated charge, obtained by combining (20) and (8) using Ohm's law, is

$$\frac{\tau_t}{\varepsilon_0} = 2\,\frac{\sigma_1 - \sigma_2}{\sigma_2 + \sigma_1}\,\mathbf{E}_b \cdot \hat{\mathbf{n}}. \tag{21}$$

The normal components of the electric field in (20) are then

$$E_{1n} = \frac{2\sigma_2}{\sigma_1 + \sigma_2}\,\mathbf{E}_b \cdot \hat{\mathbf{n}}$$

and (22)

$$E_{2n} = \frac{2\sigma_1}{\sigma_1 + \sigma_2}\,\mathbf{E}_b \cdot \hat{\mathbf{n}}.$$

The tangential component at the boundary is unaltered by the charge density and is equal to E_{bt}. Using (22), we obtain

$$\tan\theta_1 = \frac{\sigma_1 + \sigma_2}{2\sigma_2}\,\frac{E_{bt}}{E_{bn}},$$

$$\tan\theta_2 = \frac{\sigma_1 + \sigma_2}{2\sigma_1}\,\frac{E_{bt}}{E_{bn}},$$

and therefore

$$\frac{1}{\sigma_1} \tan \theta_1 = \frac{1}{\sigma_2} \tan \theta_2 . \tag{23}$$

This shows that a current line refracts as it crosses an interface; it bends towards the normal when entering a resistive medium and, conversely, it bends away from the normal when entering a conductive medium. Equation (23) is identical to the usual refraction formula (e.g. Keller and Frischknecht 1966; Telford *et al.* 1976) which is derived directly from the continuity conditions of the electric field and current density. The derivation here shows that the charge buildup on the boundary causes a change in the normal component of the electric field so that the direction of current flow is altered as it passes into a medium with different conductivity. In general, the electric field at any point within the medium is a vectorial sum of the primary field and the field produced by the accumulated charge. It is this additional field which changes the direction of current flow in the medium and results in the channelling of the current into conductive regions and the deflection away from resistive regions.

An Integral Equation for the Charge Density

Charge accumulation plays a fundamental role in d.c. resistivity problems and we therefore need a technique to quantify explicitly that role and to illustrate how it can be applied in practice. An integral equation is a desirable tool because it enables us to examine quantitatively the charge that has accumulated and it also provides an effective way to carry out the forward modelling of d.c. responses. This latter aspect has been studied by many authors (e.g. Dieter *et al.* 1969; Snyder 1976; Okabe 1984). We now develop an integral equation for charge densities which closely follows that presented by Snyder (1976).

We begin with the initial differential equation (13) and Green's second identity

$$\iiint_V (\phi \nabla^2 G - G \nabla^2 \phi) \, dv = \oiint_S \left(\phi \frac{\partial G}{\partial n} - G \frac{\partial \phi}{\partial n} \right) ds. \tag{24}$$

Green's identity is valid for any functions ϕ and G which are continuous and have derivatives up to the second order. In our case, we choose ϕ to be the potential function, satisfying (13), and G to be the whole-space Green's function

$$G(\mathbf{r}, \mathbf{r}') = \frac{1}{|\mathbf{r} - \mathbf{r}'|},$$

which satisfies

$$\nabla^2 G(\mathbf{r}, \mathbf{r}') = -4\pi\delta(\mathbf{r} - \mathbf{r}').$$

Within V, both ϕ and G decrease as inverse distance from the source and $\partial\phi/\partial n$ and $\partial G/\partial n$ decrease at least as inverse distance squared. Therefore, if S is taken as the

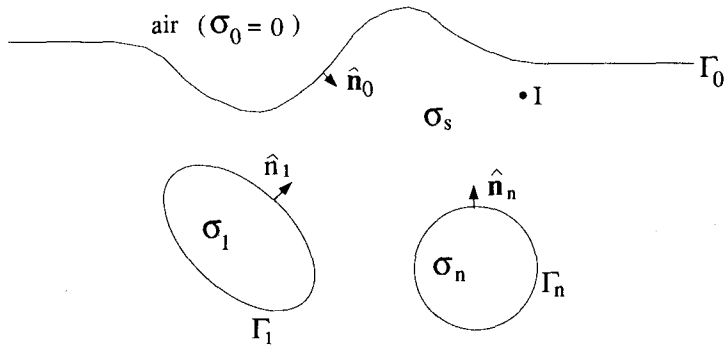

FIG. 3. The geo-electrical model consisting of n buried bodies in a uniform background beneath topography.

surface of a sphere with radius approaching infinity, the right-hand side of (24) vanishes. Substituting (13) into (24) yields

$$\phi(\mathbf{r}) = \frac{I}{4\pi\sigma_s} G(\mathbf{r}, \mathbf{r}_s) + \frac{1}{4\pi}\iiint_V \frac{\nabla\sigma(\mathbf{r}') \cdot \nabla\phi(\mathbf{r}')}{\sigma} G(\mathbf{r}, \mathbf{r}')\, dv, \tag{25}$$

where σ_s is the conductivity at the current source location. We recognize the first term in (25) as the potential due to the point source in a uniform background of conductivity σ_s. The second term is the potential due to the accumulated charge distribution.

Although (25) can be used directly, it is simpler to assume that the conductivity structure is piecewise constant. Then $\nabla\sigma$ is zero everywhere except at boundaries between regions of different conductivities. The volume integral reduces to a set of surface integrals and the integrands contain the surface charge density.

Consider the geo-electrical model shown in Fig. 3. The background medium has a conductivity σ_s. There are $n + 1$ inhomogeneities embedded in this background; each has a constant conductivity σ_i and boundary Γ_i. The zeroth inhomogeneity represents the volume of air above the earth and is bounded by the surface Γ_0. All boundaries are assumed to be piecewise smooth and $\hat{\mathbf{n}}_i$ is the outward pointing normal vector. The point current source is located in the background medium.

For this model, (25) becomes

$$\phi(\mathbf{r}) = \frac{I}{4\pi\sigma_s} G(\mathbf{r}, \mathbf{r}_s) + \frac{1}{4\pi}\sum_{i=0}^{n}\iint_{\Gamma_i} \frac{\tau_i(\mathbf{r}')}{\varepsilon_0} G(\mathbf{r}, \mathbf{r}')\, ds, \tag{26}$$

where τ_i is the charge density on the ith boundary. Using (15) and writing the normal component of the electric field in the background as $E_n = -\hat{\mathbf{n}}_j \cdot \nabla\phi$, we have

$$\frac{\tau_j}{\varepsilon_0} = \frac{\sigma_s - \sigma_j}{\sigma_j} \hat{\mathbf{n}}_j \cdot \nabla\phi. \tag{27}$$

Equation (26) is valid everywhere, so we can substitute (26) into (27) to eliminate ϕ and obtain the integral equation for τ_j:

$$\frac{\sigma_j}{\sigma_s - \sigma_j} \cdot \frac{\tau_j(\mathbf{r})}{\varepsilon_0} = \frac{I}{4\pi\sigma_s} \hat{\mathbf{n}}_j \cdot \nabla G(\mathbf{r}, \mathbf{r}_s) + \frac{1}{4\pi} \sum_{i=0}^{n} \iint_{\Gamma_i} \frac{\tau_i(\mathbf{r}')}{\varepsilon_0} \hat{\mathbf{n}}_j \cdot \nabla G(\mathbf{r}, \mathbf{r}') \, ds, \quad j = 0, \ldots, n. \tag{28}$$

Here $\mathbf{r} \in \Gamma_j$, $\hat{\mathbf{n}}_j = \hat{\mathbf{n}}_j(\mathbf{r})$, ∇ operates on the field point $\mathbf{r}$, and the integrals operate on the secondary source points $\mathbf{r}'$.

The integral over Γ_j is not straightforward to compute because the integrand in (28) is infinite when $\mathbf{r}' \to \mathbf{r}$. This singularity however is removable. A circle of radius δ centred at $\mathbf{r}$ divides Γ_j into two parts: let Γ_δ denote the area inside the circle and let Γ_j' be the area outside. This is always possible if δ is sufficiently small since we assume that the boundaries are all piecewise smooth. As $\delta \to 0$, the charge density in Γ_δ can be taken as constant and therefore,

$$\lim_{\delta \to 0} \iint_{\Gamma_\delta} \frac{\tau_j(\mathbf{r}')}{\varepsilon_0} \hat{\mathbf{n}}_j \cdot \nabla G(\mathbf{r}, \mathbf{r}') \, ds = -2\pi \frac{\tau_j(\mathbf{r})}{\varepsilon_0}.$$

Thus (28) becomes

$$\frac{\tau_j(\mathbf{r})}{\varepsilon_0} = \frac{Ik_j}{2\pi\sigma_s} \hat{\mathbf{n}}_j \cdot \nabla G(\mathbf{r}, \mathbf{r}_s) + \frac{k_j}{2\pi} \sum_{\substack{i=0 \\ i \neq j}}^{n} \iint_{\Gamma_i} \frac{\tau_i(\mathbf{r}')}{\varepsilon_0} \hat{\mathbf{n}}_j \cdot \nabla G(\mathbf{r}, \mathbf{r}') \, ds + \frac{k_j}{2\pi} \iint_{\Gamma_j'} \frac{\tau_j(\mathbf{r}')}{\varepsilon_0} \hat{\mathbf{n}}_j \cdot \nabla G(\mathbf{r}, \mathbf{r}') \, ds, \quad j = 0, \ldots, n \tag{29}$$

where $k_j = (\sigma_s - \sigma_j)/(\sigma_s + \sigma_j)$ and Γ_j' is the jth boundary with a small area around point $\mathbf{r}$ excluded. All integrals in (29) are now proper.

Equation (29) is a Fredholm equation of the second kind and is solved using standard techniques to generate the charge density on all boundaries. The potential is then evaluated by substituting these charge densities into (26).

Effect of Charge Density at the Earth's Surface

The formulation thus far has been to solve for the potential in a whole-space. This generality is advantageous because we wish ultimately to solve for the potential in the presence of surface topography. With the whole-space formulation the undulating surface may be considered to be the boundary of another body and the surface charge due to a point source can be evaluated directly.

Most work in the literature assumes a half-space model with a flat upper surface. Under such an assumption, the charge density at the earth's surface does not appear in the formulation and is equivalently taken into account by a zero flux boundary condition. Although an integral equation which incorporates the zero vertical flux of current at the earth's surface can be derived (Snyder 1976), further insight regarding the fundamental nature of the surface charges is obtained by using (29) to compute

the charge density on the surface of a flat earth and then to compute the effect of this charge distribution on the charges of buried bodies. We shall see that the effect of the charge distribution at the earth's surface can be completely reproduced by a distribution of fictitious images in the atmosphere.

We adopt a right-handed Cartesian coordinate system with z positive downward and $z = 0$ denoting the earth's surface. The coordinates of the current source are (x_s, y_s, z_s). From (29), the charge density on the earth's surface is

$$\frac{\tau_0(\mathbf{r})}{\varepsilon_0} = \frac{I}{2\pi\sigma_s} \frac{z_s}{((x - x_s)^2 + (y - y_s)^2 + z_s^2)^{3/2}} + \frac{1}{2\pi} \sum_{i=1}^{n} \iint_{\Gamma_i} \frac{\tau_i(\mathbf{r}')}{\varepsilon_0} \frac{z'}{((x - x')^2 + (y - y')^2 + z'^2)^{3/2}} \, ds. \tag{30}$$

The integral term over the earth's surface (Γ_0) does not appear in (30) because $\nabla G(\mathbf{r}, \mathbf{r}')$ is perpendicular to the surface normal. Writing (29) to isolate $\tau_0(\mathbf{r})$, and specifying a flat earth's surface, yields

$$\frac{\tau_j(\mathbf{r})}{\varepsilon_0} = \frac{Ik_j}{2\pi\sigma_s} \hat{\mathbf{n}}_j \cdot \nabla G(\mathbf{r}, \mathbf{r}_s) + \frac{k_j}{2\pi} \sum_{\substack{i=1 \\ i \neq j}}^{n} \iint_{\Gamma_i} \frac{\tau_i(\mathbf{r}')}{\varepsilon_0} \hat{\mathbf{n}}_j \cdot \nabla G(\mathbf{r}, \mathbf{r}') \, ds + \frac{k_j}{2\pi} \iint_{\Gamma_j} \frac{\tau_j(\mathbf{r}')}{\varepsilon_0} \hat{\mathbf{n}}_j \cdot \nabla G(\mathbf{r}, \mathbf{r}') \, ds + \frac{k_j}{2\pi} \int_{-\infty}^{\infty} \int_{-\infty}^{\infty} \tau_0(\mathbf{r}') \hat{\mathbf{n}}_j \cdot \nabla G(\mathbf{r}, \mathbf{r}') \, dx \, dy. \tag{31}$$

Let β_j be the last term in the above equation. Substituting (30) into β_j and applying the integral identity (Stevenson 1934),

$$\int_{-\infty}^{\infty} \int_{-\infty}^{\infty} \frac{z_1}{((x_1 - x)^2 + (y_1 - y)^2 + z_1^2)^{3/2}} \frac{1}{((x_2 - x)^2 + (y_2 - y)^2 + z^2)^{1/2}} \, dx \, dy = \frac{2\pi}{((x_1 - x_2)^2 + (y_1 - y_2)^2 + (z_1 + |z|)^2)^{1/2}}, \quad \text{for } z_1 > 0 \tag{32}$$

yields

$$\beta_j = \frac{Ik_j}{2\pi\sigma_s} \hat{\mathbf{n}}_j \nabla G(\mathbf{r}, \mathbf{r}_s') + \frac{k_j}{2\pi} \sum_{i=1}^{n} \iint_{\Gamma_i} \frac{\tau_i(\mathbf{r}')}{\varepsilon_0} \hat{\mathbf{n}}_j \cdot \nabla G(\mathbf{r}, \mathbf{r}'') \, ds, \tag{33}$$

where $\mathbf{r}_s'$ and $\mathbf{r}''$ are, respectively, the images of $\mathbf{r}_s$ and $\mathbf{r}'$ about the surface plane. The first term in (33) is recognized as the effect of a primary source at the image location $\mathbf{r}_s'$ and the second term is the effect of image bodies above the earth's surface. The final expression, obtained by combining (31) and (33), is

$$\frac{\tau_j(\mathbf{r})}{\varepsilon_0} = \frac{Ik_j}{2\pi\sigma_s} \hat{\mathbf{n}}_j \cdot \nabla \left(\frac{1}{|\mathbf{r} - \mathbf{r}_s|} + \frac{1}{|\mathbf{r} - \mathbf{r}_s'|} \right) + \frac{k_j}{2\pi} \sum_{\substack{i=1 \\ i \neq j}}^{n} \iint_{\Gamma_i} \frac{\tau_i(\mathbf{r}')}{\varepsilon_0} \hat{\mathbf{n}}_j \cdot \nabla \frac{1}{|\mathbf{r} - \mathbf{r}'|} \, ds + \frac{k_j}{2\pi} \iint_{\Gamma_j} \frac{\tau_j(\mathbf{r}')}{\varepsilon_0} \hat{\mathbf{n}}_j \cdot \nabla \frac{1}{|\mathbf{r} - \mathbf{r}'|} \, ds + \frac{k_j}{2\pi} \sum_{i=1}^{n} \iint_{\Gamma_i} \frac{\tau_i(\mathbf{r}')}{\varepsilon_0} \hat{\mathbf{n}}_j \cdot \nabla G(\mathbf{r}, \mathbf{r}'') \, ds. \tag{34}$$

This is the same equation as that of Snyder (1976), which is derived through formulating the potential problem in a half-space and using the half-space Green's function.

The whole-space and half-space Green's function approaches to calculating the charge densities are essentially equivalent. They differ in that (29) is slightly more general and can be used to treat topographic problems, whereas (34) is specifically suited to plane surface problems and is numerically more efficient in such cases.

Analytic Examples of Charge Accumulation

Generally the solution of (29) demands numerical techniques but there are a few simple geometries in which analytic solutions for the charge density are available. Here we present analyses for a point current source buried in a half-space, and a point source in a layer which overlies a half-space. These examples provide enhanced insight into the manner in which charges are distributed on various surfaces and they also provide a foundation for understanding the relationship between the solution to potential problems via charge distribution and via the image method.

1. *A point source in a half-space*

Consider a point current source at location (x_s, y_s, d) in a uniform half-space of conductivity σ_1. The charge density at the earth's surface, obtained by evaluating (29) directly, is

$$\frac{\tau(x, y)}{\varepsilon_0} = \frac{I}{2\pi\sigma_1} \frac{d}{((x - x_s)^2 + (y - y_s)^2 + d^2)^{3/2}}. \tag{35}$$

We see that $\tau(x, y)$ attains its maximum at a point directly above the current source and that its amplitude falls off as $1/|\mathbf{r} - \mathbf{r}_s|^3$. As the current source moves closer to the surface, the charge density becomes more concentrated, and we obtain

$$\lim_{d \to 0} \frac{1}{2\pi} \frac{d}{((x - x_s)^2 + (y - y_s)^2 + d^2)^{3/2}} = \delta(x - x_s)\delta(y - y_s), \tag{36}$$

and therefore

$$\lim_{d \to 0} \frac{\tau(x, y)}{\varepsilon_0} = \frac{I}{\sigma_1} \delta(x - x_s)\delta(y - y_s).$$

Substituting this charge density into (26) yields the total potential

$$\phi(\mathbf{r}) = \frac{I}{2\pi\sigma_1 |\mathbf{r} - \mathbf{r}_s|}. \tag{37}$$

This potential is double the whole-space primary potential and shows that, for a current source at the surface of a flat earth, the surface charge density provides an additional potential which is of equal strength to the whole-space primary potential.

In problems formulated explicitly as half-space problems, it is convenient to regard (37) as the primary potential.

2. *A point source in a layer over a half-space*

As the second example, we evaluate the charge distributions when a point source is located at depth d inside a layer of thickness h, overlying a half-space (Fig. 4). We adopt the same coordinate system as before, and to be consistent with the previous section, we take the layer in which the current source is located as the background medium and choose normals as shown in Fig. 4. At the boundaries Γ_0 and Γ_1,

$$k_0 = 1$$

and

$$k_1 = \frac{\sigma_1 - \sigma_2}{\sigma_1 + \sigma_2}.$$

To find the charge densities τ_0 and τ_1 on these surfaces we employ (29) in an iterative manner. We first write (29) as

$$\frac{\tau_j^{(l)}(\mathbf{r})}{\varepsilon_0} = \frac{Ik_j}{2\pi\sigma_1}\hat{\mathbf{n}}_j \cdot \nabla G(\mathbf{r}, \mathbf{r}') \qquad i = 1 \text{ when } j = 0$$

$$i = 0 \text{ when } j = 1 \qquad (38)$$

$$+ \frac{k_j}{2\pi}\iint_{\Gamma_i} \frac{\tau_i^{(l-1)}(\mathbf{r}')}{\varepsilon_0}\hat{\mathbf{n}}_j \cdot \nabla G(\mathbf{r}, \mathbf{r}')\, ds, \qquad l = 1, \ldots, \infty$$

where l denotes the iteration number. When $l = 0$, the second term on the right-hand side vanishes and the estimated charge densities are those due to the primary potential. We obtain

$$\frac{\tau_0^{(0)}}{\varepsilon_0} = \frac{I}{2\pi\sigma_1}\frac{d}{(\eta^2 + d^2)^{3/2}}$$

and (39)

$$\frac{\tau_1^{(0)}}{\varepsilon_0} = \frac{Ik_1}{2\pi\sigma_1}\frac{d}{(\eta^2 + (h-d)^2)^{3/2}},$$

where $\eta = ((x - x_s)^2 + (y - y_s)^2)^{1/2}$ is the radial distance from the source point.

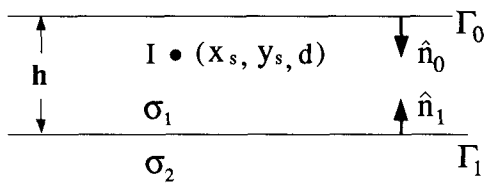

FIG. 4. A point source in a layer over a half-space. The normal vectors of the two boundaries are defined as pointing into background medium σ_1.

The presence of the primary charge distribution on Γ_0 affects the charge on Γ_1 (and vice versa); the next iteration attempts to account for this. Employing the integral identity (32) again, we obtain

$$\frac{\tau_0^{(1)}(\eta)}{\varepsilon_0} = \frac{\tau_0^{(0)}(\eta)}{\varepsilon_0} + \frac{Ik_1}{2\pi\sigma_1} \frac{2h-d}{(\eta^2 + (2h-d)^2)^{3/2}} \tag{40}$$

and

$$\frac{\tau_1^{(1)}(\eta)}{\varepsilon_0} = \frac{\tau_1^{(0)}(\eta)}{\varepsilon_0} + \frac{Ik_1}{2\pi\sigma_1} \frac{h+d}{(\eta^2 + (h+d)^2)^{3/2}}. \tag{41}$$

Proceeding with this iterative process we obtain the final solutions of charge density as series summations:

$$\frac{\tau_0(\eta)}{\varepsilon_0} = \frac{I}{2\pi\sigma_1} \frac{d}{(\eta^2 + d^2)^{3/2}} + \frac{I}{2\pi\sigma_1} \sum_{n=1}^{\infty} k_1^n \left(\frac{2nh-d}{(\eta^2 + (2nh-d)^2))^{3/2}} + \frac{2nh+d}{(\eta^2 + (2nh+d)^2)^{3/2}} \right) \tag{42}$$

and

$$\frac{\tau_1(\eta)}{\varepsilon_0} = \frac{Ik_1}{2\pi\sigma_1} \frac{h-d}{(\eta^2 + (h-d)^2)^{3/2}} + \frac{I}{2\pi\sigma_1} \sum_{n=1}^{\infty} k_1^n \left(\frac{2nh-(h-d)}{(\eta^2 + (2nh-(h-d))^2)^{3/2}} + k_1 \frac{2nh+h-d}{(\eta^2 + (2nh+h-d)^2)^{3/2}} \right). \tag{43}$$

The charge densities are observed to have maximum magnitude at $\eta = 0$, i.e. just above and below the current electrode. Away from the central point the charge density decreases in magnitude but the rate of decrease depends upon the magnitude of k_1. As $|k_1|$ becomes larger the charges are spread further over the interface. It is clear from the two formulae that the interaction between the charges on the upper and lower boundaries is primarily controlled by the magnitude of k_1 and the thickness of the layer.

As the current source approaches the surface, i.e. as $d \to 0$, a delta-like charge distribution will appear on the surface coinciding with the current source. In addition, there is a charge density

$$\Delta\tau(\eta) = \frac{I}{\pi\sigma_1} \sum_{n=1}^{\infty} k_1^n \frac{2nh}{(\eta^2 + (2nh)^2)^{3/2}},$$

which is due to the interaction with the bottom of the layer. This charge distribution can be positive or negative depending upon whether the half-space is more resistive or less resistive than the layer.

Examining (42) and (43), we notice that every term has the form of (35); that is, each term is like the charge density on a single plane interface induced by a point source. Furthermore, applying (32) to calculate the potential due to each of these

terms, results in a potential which is the same as that produced by a point charge at a certain distance away from the interface. This leads to the understanding of the physical basis for the image method solution of potential problems.

Image Method in Terms of Charge Accumulation

We consider the first example shown in the last section and increase the generality slightly by allowing the upper half-space to have finite conductivity σ_0. The charge density along the interface, obtained by evaluating (29), is

$$\frac{\tau(x, y)}{\varepsilon_0} = \frac{Ik}{2\pi\sigma_1} \frac{d}{((x - x_s)^2 + (y - y_s)^2 + d^2)^{3/2}}, \tag{44}$$

where $k = (\sigma_1 - \sigma_0)/(\sigma_1 + \sigma_0)$. As $\sigma_0 \to 0$ we obtain the special case of the half-space whose charge density is given by (35).

The potential anywhere in the whole-space is the sum of the primary potential from the current source and the secondary potential due to the charges on the interface. Evaluating (26) and using identity (32) yields

$$\phi(x, y, z) = \frac{I}{4\pi\sigma_1} \frac{1}{R} + \frac{Ik}{4\pi\sigma_1} \frac{1}{((x - x_s)^2 + (y - y_s)^2 + (d + |z|)^2)^{1/2}},$$

where $R = ((x - x_s)^2 + (y - y_s)^2 + (z - d)^2)^{1/2}$. Thus the potential in the lower medium, where $z > 0$, is

$$\phi_1 = \frac{I}{4\pi\sigma_1} \left(\frac{1}{R} + \frac{k}{R'} \right), \tag{45}$$

where $R' = ((x - x_s)^2 + (y - y_s)^2 + (z + d)^2)^{1/2}$. This potential is equivalent to that arising from a current of strength I located at R and another current of strength kI located at R'. In the upper medium, where $z < 0$, the potential may be written as

$$\begin{aligned} \phi_2 &= \frac{I}{4\pi\sigma_1} \frac{1 + k}{R''} \\ &= \frac{I}{4\pi\sigma_0} \frac{t}{R''}, \end{aligned} \tag{46}$$

where $R'' = ((x - x_s)^2 + (y - y_s)^2 + (z - d)^2)^{1/2}$ and $t = 2\sigma_0/(\sigma_1 + \sigma_0)$. The second form of the potential in (46) is equivalent to that produced by a current of strength tI at a distance R'' in a whole-space of conductivity σ_0. Equations (45) and (46) are identical to those derived from the image method by Keller and Frischknecht (1966) and Telford *et al.* (1976), where an analogy is drawn between electric current flow and geometrical optics, based on the fact that the intensity of both current density and light emanating from a point source varies as the inverse square of distance. The plane interface between two media is viewed as a semitransparent mirror. Based on this analogy, t and k defined above are referred to as transmission and reflection coefficients, respectively. Although the correct equations are derived using the geometrical optics formula, the physical understanding is not present. Our derivation

has explicitly shown that the image method has worked because it was possible to find a fictitious point charge which produced the same potential as the true distribution of charges on the boundary.

Although the whole-space single interface example establishes the basic principles of the image method, a slightly more complicated model is required so that internal interactions can be modelled. Correspondingly, we consider the structure in Fig. 4 with the current source moved to the surface. From (42) and (43), the charge densities on the upper and lower surfaces are

$$\frac{\tau_0(x, y)}{\varepsilon_0} = \frac{I}{\sigma_1}\delta(x - x_s)\delta(y - y_s) + \frac{I}{\pi\sigma_1}\sum_{n=1}^{\infty} k^n \frac{2nh}{(\eta^2 + (2nh)^2)^{3/2}}, \tag{47}$$

and

$$\frac{\tau_1(x, y)}{\varepsilon_0} = \frac{I}{\pi\sigma_1}\sum_{n=1}^{\infty} k^{n+1} \frac{(2n+1)h}{((\eta^2 + ((2n+1)h)^2)^{3/2}}, \tag{48}$$

where $k = (\sigma_1 - \sigma_2)/(\sigma_1 + \sigma_2)$. By evaluating (26), the potential at any point in the space is

$$\begin{aligned}\phi(x, y, z) = {} & \frac{I}{2\pi\sigma_1 R} \\ & + \frac{I}{2\pi\sigma_1}\sum_{n=1}^{\infty} \frac{k^n}{((\eta^2 + (2nh + |z|)^2)^{1/2}} \\ & + \frac{I}{2\pi\sigma_1}\sum_{n=0}^{\infty} \frac{k^{n+1}}{((\eta^2 + ((2n+1)h + |z - h|)^2)^{1/2}},\end{aligned} \tag{49}$$

where $\eta = ((x - x_s)^2 + (y - y_s)^2)^{1/2}$. Equation (49) is identical to that derived using image methods, for which one needs to compute potentials due to two families of image sources (see Keller and Frischknecht 1966, pp. 108–111 for a detailed treatment).

To summarize our statements concerning the relationship between the charge density and the image solution we return to (48). τ_1 represents the charge that is accumulated on the interface between the layer and the underlying half-space. The potential due to this charge is obtained by integrating with the whole-space Green's function, i.e.

$$\Delta\phi(\mathbf{r}') = \frac{1}{4\pi\varepsilon_0}\iint_{\Gamma_1} \tau_1(\mathbf{r}')\frac{1}{|\mathbf{r} - \mathbf{r}'|}\,ds, \tag{50}$$

at any position $\mathbf{r}$ in the medium. The image method reproduces the same potential through a series solution (the second summation in (49)). We recognize each term in the series as being the potential due to a point charge located in the half-space and beneath the primary current location. Thus whereas $\Delta\phi$ in (50) is obtained by the integration of a real charge distribution on the boundary, the series summation produces the same result by employing a set of fictitious image sources. Therefore the essence of the image method solution to the potential problem is to derive a set

of fictitious sources which produce the same potential as does the true charge distribution. It follows that the image method is viable only when the conductivity structure is such that the effect of the accumulated charge can be represented by a set of point images.

The image method is not applicable to all problems. In general, potentials from all 1D conductivity functions can be found using images. The derivation are simplified if the earth is represented as a series of homogeneous layers of constant thickness h_0. There is no loss of generality in doing this since h_0 can be made small and adjacent layers need not have different conductivities. With such a representation, the potential solution has the form

$$\phi(\eta, z) = \frac{I}{2\pi\sigma_1} \int_0^\infty \sum_{n=0}^{\infty} q_n e^{-2\lambda n h_0} J_0(\lambda\eta)\, d\lambda,$$

where the q_n's are the image strengths and depend upon the reflection and transmission coefficients at the layer boundaries (Kunetz 1972; Szareniec 1976; Levy, Oldenburg and Wang 1988). Applicability of the image method to 2D or 3D problems, however, is more restricted. Alfano (1959) considered conductivity structures composed of rectangular prisms of constant conductivity bounded by two orthogonal plane interfaces. If σ_1, σ_2, σ_3, σ_4 denote the conductivities in successive quadrants defining the prisms, then Alfano proves that the image solution exists if, and only if, $\sigma_1\sigma_4 = \sigma_2\sigma_3$. Physically, this condition ensures that the charge density on each interface is continuous at the intersection point. When continuity of physical charge density exists then the potentials can be represented as arising from a set of fictitious image charges. However, when $\sigma_1\sigma_4 \neq \sigma_2\sigma_3$ the charge density is discontinuous at the intersection point, no representation of potentials by point charges is available, and the image method is not applicable.

Numerical Examples of Charge Distribution

For an arbitrarily shaped conductivity structure, the charge density on all interfaces is found by solving (29). There are many ways to solve this Fredholm integral equation but most methods first divide all interfaces into a set of small areal segments known as elements. Some representation for the charge density on each element is then assumed. Different choices are possible: the charge density may be assumed to be concentrated as a point charge located at the centre of gravity of the element; it may be assumed constant or linearly varying over the element; or it may be represented by some higher-order polynomial. Substitution of the representation for the charge density into the integral equation yields a system of linear equations to be solved (e.g. Alfano 1959; Harrington 1968; Pratt 1972; Snyder 1976; Eskola 1979; Brebbia and Walker 1980; Okabe 1984; Oppliger 1984; Shulz 1985; Das and Parasnis 1987).

As an example, consider a pure topographic problem in which a single interface Γ overlies a homogeneous medium of conductivity σ_0. The surface Γ is divided into

M elements and a constant τ_j is assigned to the jth element. Substitution into (29) yields

$$\frac{\tau_i}{\varepsilon_0} = \frac{Ik_i}{2\pi\sigma_0}\frac{\partial G(\mathbf{r}_i, \mathbf{r}_s)}{\partial n_i} + \frac{k_i}{2\pi}\sum_{\substack{j=1 \\ j\neq i}}^{M}\frac{\tau_j}{\varepsilon_0}\iint_{\Delta\Gamma_j}\frac{\partial G(\mathbf{r}_i, \mathbf{r}')}{\partial n_i}\,\mathrm{d}s, \qquad i = 1, \ldots, M \tag{51}$$

where $\mathbf{r}_i$ is the centre of gravity of the ith element, and $\tau_i = \tau(\mathbf{r}_i)$ is the charge density of this element. The integral over the ith element vanishes after the singularity is removed.

By reordering, the equations in (53) may be written in matrix form as

$$\mathbf{A}\tau = \tau^{(0)}, \tag{52}$$

where $\mathbf{A}$ is an $M \times M$ coefficient matrix with components

$$A_{ii} = 1,$$

$$A_{ij} = \frac{k_i}{2\pi}\iint_{\Delta\Gamma_j}\frac{\partial G(\mathbf{r}_i, \mathbf{r}')}{\partial n_i}\,\mathrm{d}s, \tag{53}$$

τ is the $M \times 1$ vector of the unknown charge densities and $\tau^{(0)}$ has components

$$\tau_i^{(0)} = \frac{Ik_i}{2\pi\sigma_0}\frac{\partial G(\mathbf{r}_i, \mathbf{r}_s)}{\partial n_i}. \tag{54}$$

The linear system of equations can be solved directly by decomposing the matrix $\mathbf{A}$, or it can be solved through iterative techniques.

In (52) we have denoted the right-hand side by $\tau^{(0)}$. The reason for this is that $\tau^{(0)}$ is a first-order approximation to the charge density we are seeking. It is the charge density that would exit if the potential at the boundary were equal to the primary potential. This approximation sometimes yields fairly good estimates of potential anomaly and delineates first-order characteristics (Keller and Frischknecht 1966). The computational ease with which $\tau^{(0)}$ can be evaluated makes this approximation very desirable.

To illustrate quantitatively the charge accumulation in more complicated geoelectrical structures we consider two examples. In the first, we compute the charge distribution on a surface topography overlying a uniform earth. The topographic model and the charge distribution arising when a current electrode is located in the middle of the valley are shown in Fig. 5. A negative charge is observed on the valley walls but everywhere else the charge is positive. The maximum negative charge densities occur on the wall beside the current source. Along the strike, the charge density decays with the distance away from the source. The charge distribution at the bottom of the valley is primarily a result of interaction effects with the negative charge on the valley walls.

This physical charge residing on the earth's surface produces an anomalous potential which is displayed in Fig. 5c. When that potential is added to the primary potential and converted to apparent resistivity using the formula $\rho_a(r) = 2\pi r\phi(r)/I$, we obtain the distorted apparent resistivity map shown in Fig. 5d, in which the apparent resistivities are plotted at the locations where the potential was observed.

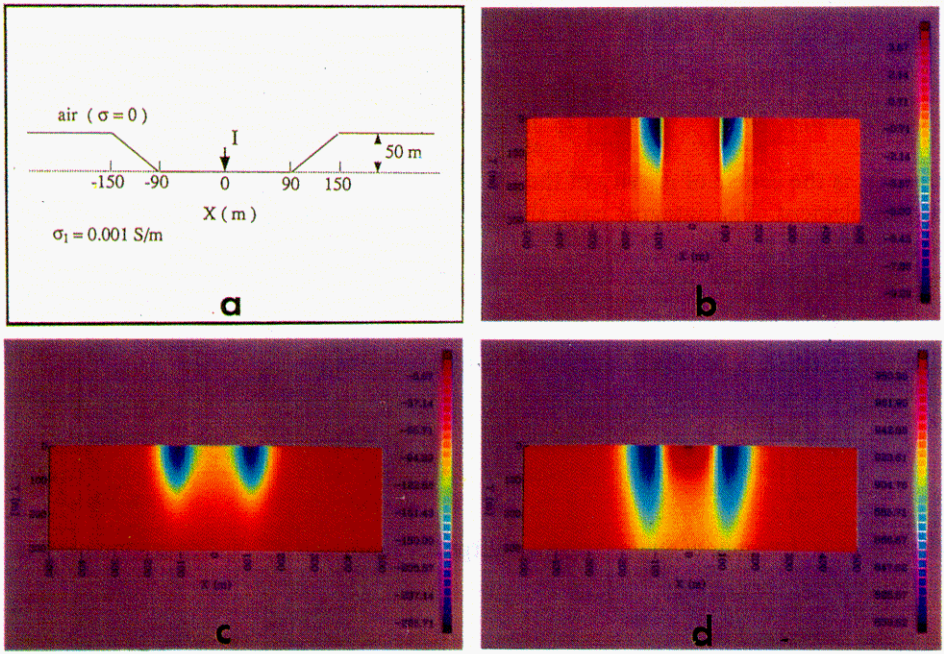

FIG. 5. The charge density on a 2D topographic surface. The geometry of the cross-section is shown in (a). The charge density on the 2D topographic surface is shown in (b). The y-coordinate delineates offsets in the strike direction. Because of symmetry only charge densities for positive value of y are shown. The surface anomalous potential is shown in (c) and the surface apparent resistivity is displayed in (d).

It is noted that the apparent resistivity in and near the topographic depression is less than the intrinsic half-space resistivity.

This example shows that the physical charge caused by topographic variation gives rise to a perturbation potential that will distort the signal of buried bodies. However, the insight afforded by this example can also be used in reverse. A correction for topographic distortions can be made by first estimating the accumulated surface charge and then subtracting the resultant potential from the field observations. This approach has been used with success by Oppliger (1984).

The second example is selected to illustrate the charge accumulation that exists on a conductive prism buried in a uniform half-space. The geometry of the structure, the charge densities on the prism, the anomalous surface potential, and the surface apparent resistivity are shown in Fig. 6. Negative charges exist on the top and left faces of the cube and this is in accordance with current flowing into the prism there. Positive charges are seen on all other faces. Near the upper left corner of the front face (and, by symmetry, on the back face), there is a small area with negative charge indicating that current is flowing into the prism in that region. This is a vivid

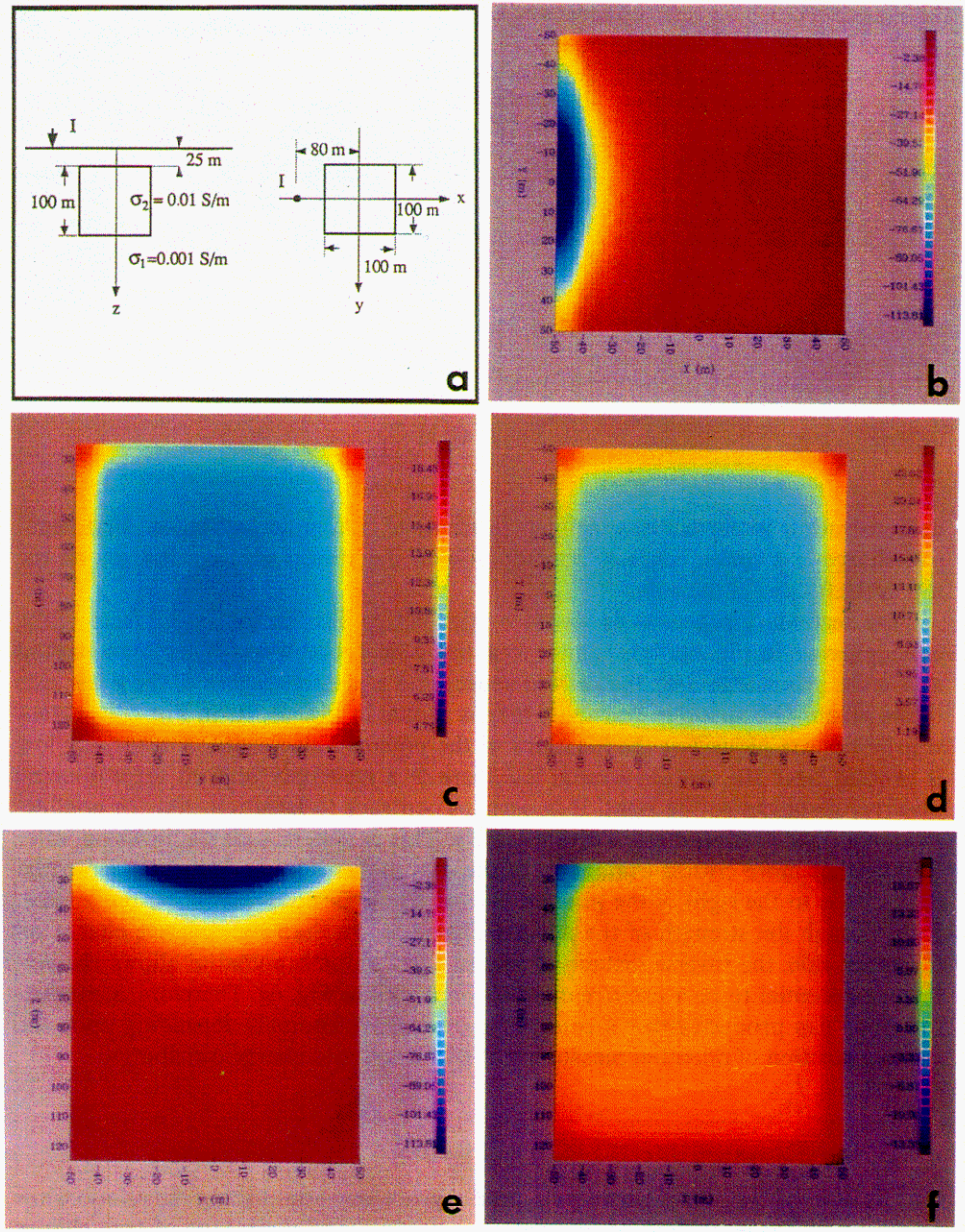

FIG. 6. The charge density on a buried prism. The geometry and conductivities are shown in (a). (b)–(f) respectively show the charge densities on the top, right, bottom, left, and front faces of the prism. The secondary potential at the surface of the earth is shown in (g) and the corresponding apparent resistivity map is shown in (h).

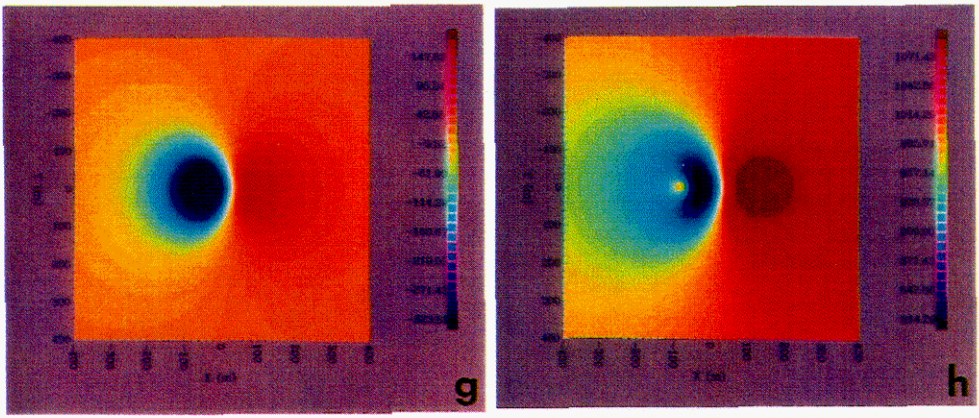

FIG. 6. (g–h)

demonstration of current channelling. In terms of charge accumulation, that negative charge is a consequence of interaction with the strong negative charges on the top and left faces of the cube.

The secondary potential produced by the charge distribution on all faces of the cube is shown in Fig. 6g. It is similar to a dipole field with a negative region centred above the prism edge near the current source and a positive region at the other side of the prism. The apparent resistivity map is shown in Fig. 6h. As in Fig. 5, apparent resistivities are plotted at the locations of the potential electrodes. A resistivity low is centred near the current source but there is a resistivity high at large source–observer distances to the right. It is perhaps contrary to intuition that the conductive prism has produced a resistive anomaly. This is understandable, however, after a somewhat more critical evaluation of the charge distribution. When the potential electrode is to the right of the prism it is close to the positive charge on those faces. Even though the strength of the positive charge is less than the negative charge on the other side, the inverse distance decay in the Coulomb potential allows the secondary potential to be a positive quantity as shown in Fig. 6g. Therefore, a conductive body can produce either a conductive or resistive anomaly depending upon the relative position of potential measurement with respect to charge distribution.

CONCLUSION

Clarification of the role of permittivity in d.c. problems; establishing the relationship between the image method of calculating potentials and the effects of true charge accumulation; relating the effects of charge accumulation and refraction of current at a boundary separating media with different conductivities; and quantification of the charge distributions through the use of integral equations with half-space and whole-space Green's functions all provide a greater understanding of the d.c. electrical problem. However, the most important benefit of our investigation of charge

accumulations has been in understanding the observed d.c. potentials. When the geological structures are simple, it is often possible to sketch the magnitude and sign of charges on buried bodies and on the earth's surface that result from an arbitrary specification of the current source location. Thus, secondary potentials and apparent resistivity perturbations can be estimated so as to delineate essential features of the resistivity anomaly. This helps to establish an intuitive understanding of the relationship between resistivity anomalies and geo-electrical structures which is immediately useful in making preliminary interpretations of observed potentials or in making first-order judgements about the validity of results produced from numerical simulation.

ACKNOWLEDGEMENTS

The perceived need for a paper about charge density grew out of a geophysical seminar study on the d.c. resistivity problem. The arguments pertaining to the physical existence (or non-existence) of charge accumulations in the dc. problem, our inability to make physical connections between the image technique and other methods of solving the problem, and the uncertainty about the role of permittivity were catalysts for the various topics covered here. We thank D. Aldridge, E. Blake, S. Dosso, R. G. Ellis, D. Lumley and P. McGillivray for provocative discussions and insight. This work is supported by NSERC grants 5-84270 and 5-80141. One of the authors (Y.L.) is partly supported by a University of British Colombia Graduate Fellowship.

REFERENCES

ALFANO, L. 1959. Introduction to the interpretation of resistivity measurements for complicated structural conditions. *Geophysical Prospecting* **7**, 311–368.

ALFANO, L. 1960. The influence of surface formations on the apparent resistivity values in the electrical prospecting, part 1. *Geophysical Prospecting* **8**, 576–606.

ALFANO, L. 1961. The influence of surface formations on the apparent resistivity values in the electrical prospecting, part 2. *Geophysical Prospecting* **9**, 213–241.

ALPIN, L.M. 1947. Source of the field in the theory of electroprospecting by direct current. *Applied Geophysics* **3**, 57–100.

BREBBIA, C.A. and WALKER, S. 1980. *Boundary Element Techniques in Engineering.* Butterworth and Co. Ltd.

DAS, U.C. and PARASNIS, D.S. 1987. Resistivity and induced polarization responses of arbitrarily shaped 3D bodies in a two-layered earth. *Geophysical Prospecting* **35**, 98–109.

DIETER, K., PATERSON, N.R. and GRANT, F.S. 1969. IP and resistivity type curves for three-dimensional bodies. *Geophysics* **34**, 615–632.

ESKOLA, L. 1979. Calculation of galvanic effects by means of the method of sub-areas. *Geophysical Prospecting* **27**, 616–627.

GRANT, F.S. and WEST, G.F. 1965. *Interpretation Theory in Applied Geophysics.* McGraw-Hill Book Co.

HARRINGTON, R.F. 1968. *Field Computation by Momentum Methods.* The Macmillan Publishing Co., Inc.

JEANS, J.H. 1966. *The Mathematical Theory of Electricity and Magnetism.* Cambridge University Press.

KAUFMAN, A.A. 1985. Distribution of alternating electrical charges in a conducting medium. *Geophysical Prospecting* **33**, 171–184.

KAUFMAN, A.A. and KELLER, G.V. 1985. *Inductive Mining Prospecting.* Elsevier Science Publishing Co.

KELLER, G.V. and FRISCHKNECHT, F.C. 1966. *Electrical Methods in Geophysical Prospecting.* Pergamon Press Inc.

KUNETZ, G. 1972. Processing and interpretation of magnetotelluric soundings. *Geophysics* **37**, 1005–1021.

LEVY, S., OLDENBURG, D. and WANG, J. 1988. Subsurface imaging using magnetotelluric data. *Geophysics* **53**, 104–117.

OKABE, M. 1984. Boundary element method for the arbitary inhomogeneities problem in electrical prospecting. *Geophysical Prospecting* **29**, 39–59.

OPPLIGER, G.L. 1984. Three-dimensional terrain corrections for mise-à-la-masse and magnetometric resistivity surveys. *Geophysics* **49**, 1718–1729.

PRATT, D.A. 1972. The surface integral approach to the solution of the 3D resistivity problems, ASEG *Bulletin* **3**, 33–50.

SHULZ, R. 1985. The method of integral equation in the direct current resistivity method and its accuracy. *Journal of Geophysics* **56**, 192–200.

SNYDER, D.D. 1976. A method for modelling the resistivity and IP responses of two-dimensional bodies. *Geophysics* **41**, 997–1015.

STEVENSON, A.F. 1934. On the theoretical determination of earth resistance from surface potential measurements. *Physics* **5**, 114–124.

STRATTON, J.A. 1941. *Electromagnetic Theory.* McGraw-Hill Book Co.

SZARANIEC, E. 1976. Fundamental functions for horizontally stratified earth. *Geophysical Prospecting* **24**, 528–548.

TELFORD, W.M., GELDART, L.P., SHERIFF, R.E. and KEYS, D.A. 1976. *Applied Geophysics.* Cambridge University Press.

WARD, S.H. and HOHMANN, G.W. 1988. *Electromagnetic Method in Applied Geophysics – Theory*, Chapter 4. M. N. Nabighian ed., Society of Exploration Geophysicists, Tulsa.